Cell

Polycomb-Dependent Regulatory Contacts between Distant Hox Loci in *Drosophila*

Frédéric Bantignies,[1,3,*] Virginie Roure,[1,3,4] Itys Comet,[1,5] Benjamin Leblanc,[1] Bernd Schuettengruber,[1] Jérôme Bonnet,[1,6] Vanessa Tixier,[1,7] André Mas,[2] and Giacomo Cavalli[1,*]
[1]Institut de Génétique Humaine, CNRS UPR 1142, 141, rue de la Cardonille, 34396 Montpellier Cedex 5, France
[2]Institut de Modélisation Mathématique de Montpellier, CNRS UMR 5149, Université Montpellier 2, Place Eugène Bataillon, 34095 Montpellier Cedex 5, France
[3]These authors contributed equally to this work
[4]Present address: Max-Planck Institute of Immunobiology, Stübeweg 51, D-79108 Freiburg, Germany
[5]Present address: Biotech Research & Innovation Centre, University of Copenhagen, Ole Maaløes Vej 5, DK-2200 Copenhagen N, Denmark
[6]Present address: Department of Bioengineering, Stanford University, Stanford, CA 93405, USA
[7]Present address: Unité de Génétique, Reproduction et Développement, INSERM-CNRS UMR 6247, Université de Clermont-Ferrand, 28 Place Henri Dunant, 63000 Clermont-Ferrand, France
*Correspondence: frederic.bantignies@igh.cnrs.fr (F.B.), giacomo.cavalli@igh.cnrs.fr (G.C.)
DOI 10.1016/j.cell.2010.12.026

SUMMARY

In *Drosophila melanogaster,* Hox genes are organized in an anterior and a posterior cluster, called Antennapedia complex and bithorax complex, located on the same chromosome arm and separated by 10 Mb of DNA. Both clusters are repressed by Polycomb group (PcG) proteins. Here, we show that genes of the two Hox complexes can interact within nuclear PcG bodies in tissues where they are corepressed. This colocalization increases during development and depends on PcG proteins. Hox gene contacts are conserved in the distantly related *Drosophila virilis* species and they are part of a large gene interaction network that includes other PcG target genes. Importantly, mutations on one of the loci weaken silencing of genes in the other locus, resulting in the exacerbation of homeotic phenotypes in sensitized genetic backgrounds. Thus, the three-dimensional organization of Polycomb target genes in the cell nucleus stabilizes the maintenance of epigenetic gene silencing.

INTRODUCTION

The organization of chromosomal domains in the cell nucleus plays an important role in the regulation of gene expression during cellular differentiation and development (Fraser and Bickmore, 2007; Williams et al., 2010). During interphase, eukaryotic chromosomes are organized as distinct domains called chromosome territories, which adopt specific structure and position in the cell nucleus. These territories are not strictly delimited in the nuclear space, allowing for some intermingling with other chromosomes (Branco and Pombo, 2006). It has been reported that chromosomal elements separated by large genomic distances are sometimes able to interact in the nuclear space. The phenomenon of long-range contacts between different chromosomal loci has been called "chromosome kissing" (Cavalli, 2007). Chromosome kissing has been reported for X chromosome inactivation, where the two copies come transiently in close proximity at the onset of the inactivation process (Okamoto and Heard, 2009). The same phenomenon has been observed in few other situations. However, it is not clear how these contacts may contribute to gene regulation in living organisms (Sexton et al., 2009; Williams et al., 2010).

Long-range gene regulation may involve epigenetic components including proteins of the Polycomb group (PcG) (Grimaud et al., 2006; Sexton et al., 2007). PcG proteins are organized into nuclear foci called PcG bodies (Alkema et al., 1997; Buchenau et al., 1998; Messmer et al., 1992; Ren et al., 2008; Saurin et al., 1998). These bodies contain silenced PcG target chromatin (Grimaud et al., 2006; Lanzuolo et al., 2007), which is made of multimeric PcG complexes bound to *cis*-regulatory elements named PcG response elements (PREs) (Muller and Verrijzer, 2009; Schuettengruber et al., 2007). PcG protein binding to PREs silences genes involved in developmental patterning and cell proliferation (Merdes and Paro, 2009). In *Drosophila melanogaster,* Hox genes are the most prominent PcG targets. They are organized in two complexes: the Antennapedia complex (ANT-C) spans approximately 400 kb and comprises five Hox genes (*lab*, *pb*, *Dfd*, *Scr*, and *Antp*) that specify parts of the head and the anterior thorax (Kaufman et al., 1990), while the bithorax complex (BX-C) spans approximately 350 kb and contains three Hox genes (*Ubx*, *abd-A*, and *Abd-B*) involved in the development of the posterior thorax and the abdomen (Duncan, 1987; Lewis et al., 2003). The nuclear organization of the BX-C has been studied by Fluorescent In Situ Hybridization (FISH) and Chromosome Conformation Capture (3C) approaches (Lanzuolo et al., 2007). This study revealed the existence of long-distance interactions among the major elements bound by PcG proteins, including PREs and core promoters. Importantly, upon activation of the *Abd-B* gene, its interactions with the other genes of the complex are lost. Two particular PRE-containing elements called *Fab-7* and

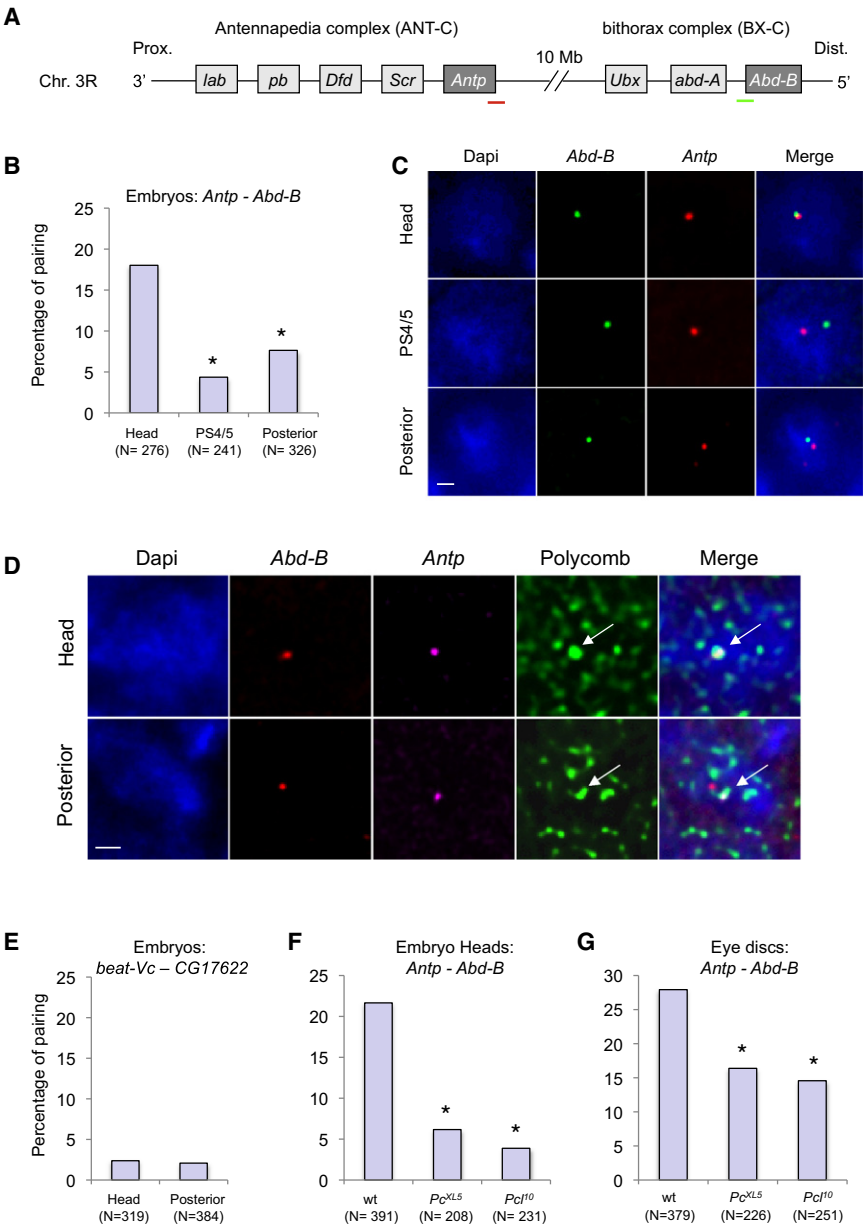

Figure 1. Kissing of Repressed Hox Genes

(A) Schematic drawing illustrating the anterior and the posterior Hox gene clusters in *D. melanogaster*. The colored lines represent the approximate localization of the FISH probes for *Antp* (red) and *Abd-B* (green).

(B) FISH in wild-type (WT) stage 10–11 embryos. Percentage colocalization between *Antp* and *Abd-B*. A maximum distance of 350 nm was used to define pairing between the two loci. The p values of the pairwise comparison are 2.045e-06 for Head versus PS4/5, 1.1e-04 for Head versus Posterior, 0.137 for PS4/5 versus Posterior.

(C) Characteristic examples of individual nuclei.

(D) FISH-I of *Abd-B, Antp* and PC. The regions chosen for image acquisition are indicated to the left. Figure images correspond to deconvolved single slices from 3D stacks. The scale bars represent 1 μm.

(E) Percentage colocalization between *beat-Vc and CG17622*, two non PcG-targets, which are located 10 Mb away on Chromosome 3R. The p value is 0.707.

(F) Percentage of colocalization between *Antp* and *Abd-B* in heads of stage 13–14 embryos from WT, Pc^{XL5} and Pcl^{10} homozygous mutants. The p values are 1.066e-06 for WT versus Pc^{XL5}, 1.936e-09 for WT versus Pcl^{10}, 0.259 for Pc^{XL5} versus Pcl^{10}.

(G) Percentage of colocalization between *Antp* and *Abd-B* in third instar larval imaginal eye discs from WT, Pc^{XL5} and Pcl^{10} heterozygous mutants. The p values are 2.3e-03 for WT versus Pc^{XL5}, 2.372e-04 for WT versus Pcl^{10}, 0.623 for Pc^{XL5} versus Pcl^{10}. N indicates the total number of nuclei analyzed in 3–5 embryos or tissues. Asterisks indicate that the pairwise difference between samples corresponding to the left column and the other samples is significant.

See also Figure S1 and Table S1.

Mcp, both involved in the regulation of *Abd-B*, have been directly implicated in chromosome kissing events when extra copies were introduced in the fly genome as transgenes. In both cases, contacts strengthen PcG-dependent gene silencing and kissing events occur specifically at PcG bodies (Bantignies et al., 2003; Grimaud et al., 2006; Muller et al., 1999; Vazquez et al., 2006), although they are clearly tissue-specific and do not occur in several larval tissues containing polytene chromosomes (Fedorova et al., 2008). These data raise the question of whether PcG bodies might be involved in the functional compartmentalization of the Hox clusters or other Polycomb target genes.

In *D. melanogaster*, the ANT-C and BX-C complexes are located on the right arm of chromosome 3 (3R), separated by approximately 10 Mb of euchromatic sequences that contain more than 1,200 annotated genes and represent more than one-third of the euchromatic fraction of 3R (Figure 1A). In this work, we provide evidence that the two distant Hox clusters can be corepressed by PcG proteins via association in three-dimensional nuclear space between the *Antennapedia* (*Antp*) gene from the ANT-C and the *Abdominal-B* (*Abd-B*) and *Ultrabithorax* (*Ubx*) genes from the BX-C. We define this phenomenon as "Hox gene kissing." Furthermore, 3C on chip (4C) confirmed Hox contacts and revealed additional *Abd-B* partner loci. Importantly, Hox gene kissing is conserved in *D. virilis*, a species evolutionarily separated from *D. melanogaster* by around 60 Myr. Moreover, we demonstrate that the BX-C element *Fab-7* participates in Hox gene kissing, and that removal of this element weakens silencing of distant genes in the ANT-C locus, indicating that PcG-dependent chromatin contacts have a functional role in stabilizing gene silencing.

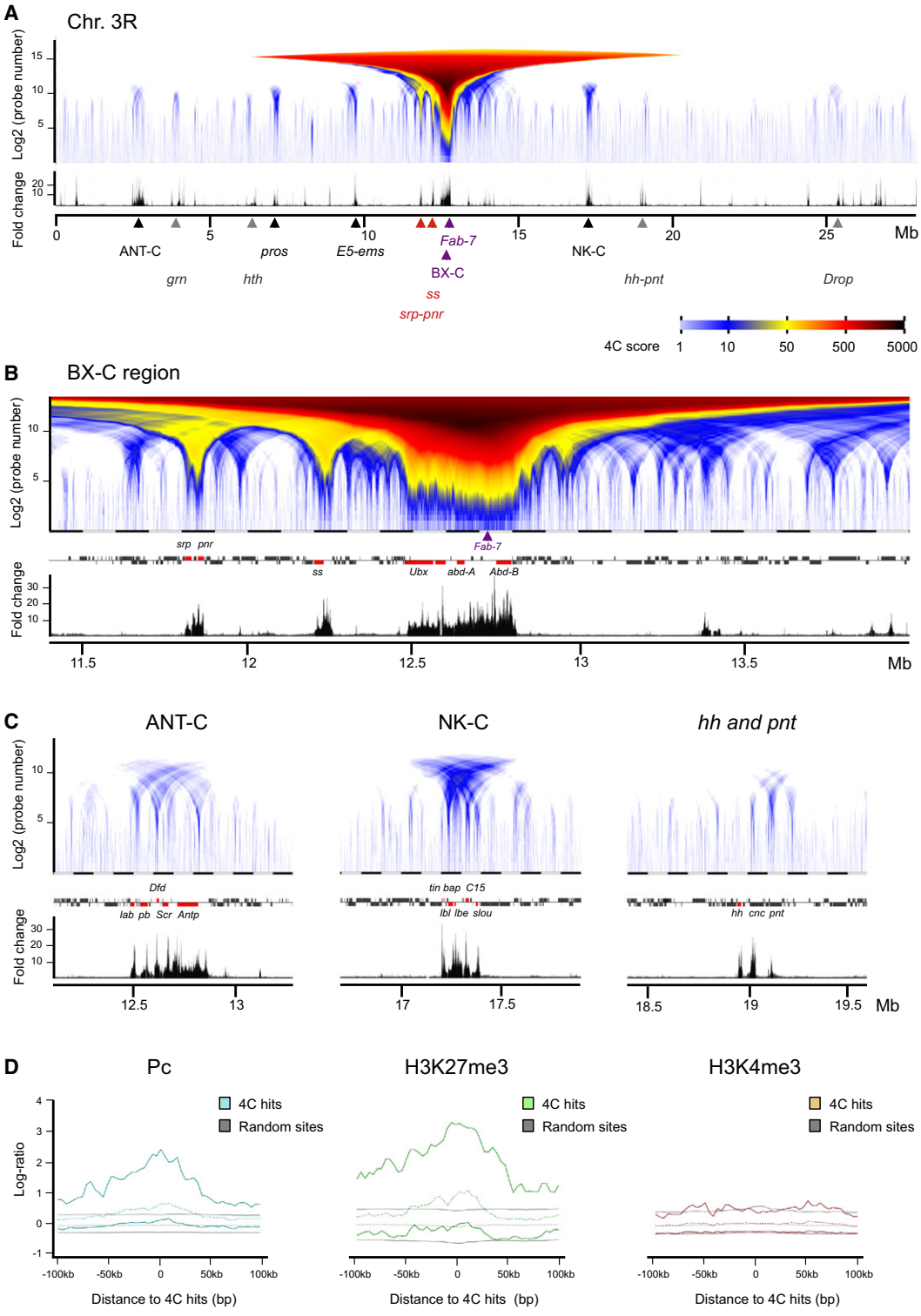

Figure 2. Extensive Interactions of the *Fab-7* Element and Other PcG Target Genes along the 3R Chromosome Arm

(A) Whole 3R chromosome domainogram representation of WT 4C profile (top) and Pc ChIP enrichments as fold change in WT 4–12 hr embryos (bottom, black). The x axis represents chromosome 3R coordinates in Mb and the y axis of the domainogram represents domain sizes as the Log2 of the number of contiguous probes involved in the calculation of statistical scores (see Figure S2H for genomic length conversion). Purple arrowheads indicate the *Fab-7* bait and the BX-C. Red arrowheads indicate strong hits within 2 Mb of the anchor region, Black arrowheads indicate the strongest long-range hits, Grey arrowheads indicate other significant long-range target regions.

RESULTS

The Nuclear Organization of the Antennapedia and Bithorax Complexes

We first analyzed the relative positioning of the two Hox complexes in the nucleus, starting with the most distal genes within each complex: *Abd-B* from the BX-C, and *Antp* from the ANT-C. We used two-color FISH in whole mount embryos and larval tissues, followed by three-dimensional image analysis (Bantignies et al., 2003). We compared embryonic and larval nuclei with different Hox gene expression profiles (Castelli-Gair, 1998; Kosman et al., 2004; Morata et al., 1994). We first focused on developmental stage 10–11, when PcG-mediated regulation of homeotic genes has already initiated (Pirrotta et al., 1995). 3D image acquisitions were carried out in ectodermal interphase diploid nuclei in three different regions along the anteroposterior axis of the embryo: the head, where both genes are repressed, a thoracic region including parasegments (PS) 4 and 5, where *Antp* is expressed and *Abd-B* repressed, and the posterior tip of the embryo (PS 13 and 14), where the reciprocal situation is observed, i.e., *Abd-B* is activated and *Antp* repressed.

Abd-B and the *Antp* gene rarely colocalized in the thoracic PS and in the posterior PS, with colocalization rates of 4% and 7.6%, respectively. In contrast, the association between the loci was significantly stronger in the head where both loci are repressed (18%, Figure 1B,C). This was reflected in a global three-dimensional distance distribution skewed toward shorter distances in the head (Table S1, available online). Later during development, the association between *Antp* and *Abd-B* was reinforced in anterior larval tissues compared to more posterior tissues such as leg and wing discs, where only *Antp* is active (Figure S1A and Table S2).

Antp also colocalized with the repressed *Ubx* gene in the head compartment of embryonic nuclei, and this interaction was lost in the trunk (PS4/5), where *Antp* is active. In the posterior PS, however, where both *Ubx* and *Antp* are repressed, they colocalized significantly more than in PS4/5 (Figures S1B and S1C and Table S2). This indicates that Hox gene kissing correlates with the repression status of both Hox genes.

Hox Gene Kissing Occurs at PcG Bodies and Depends on the Function of PcG Proteins

Next we combined FISH with immunostaining using a Polycomb antibody (FISH-I) to analyze the nuclear localization of *Antp, Abd-B*, and *Ubx* relative to PcG bodies. Repressed genes are associated with large PcG bodies in 80% to 85% of the cases. In embryo heads, where both *Antp* and *Abd-B* are colocalized, the two genes were found in the same PcG body (Figure 1D). In posterior segments, *Abd-B* is clearly outside PcG bodies in 80% of the cases (Figure 1D), although the two Hox complexes can still associate via kissing of *Antp* and *Ubx* within PcG bodies (Figure S1C). In the thoracic PS4/5, in which the *Antp* gene is activated, *Antp* is outside PcG bodies in 85% of the cases, while *Abd-B* and *Ubx* are inside (data not shown), correlating with the lack of colocalization between *Antp* and the other genes.

We then analyzed whether PcG proteins are required for Hox gene kissing. First, two non-PcG target genes, *beat-Vc* and *CG17622*, which are located on chromosome 3R and separated by 10 Mb like the Hox complexes, colocalize in less than 5% of the nuclei (Figure 1E and Table S1). Second, in the head of *Polycomb* and *Polycomb-like* mutant embryos, the *Antp* and *Abd-B* genes colocalize in about 5% of the nuclei, i.e., much less than in WT and close to the two control genes *beat-Vc* and *CG17622* (Figure 1F and Table S1). This indicates that PcG proteins are required for pairing of the two loci. Even heterozygous mutations in the *Pc* and *Pcl* genes reduced the frequency of gene kissing in anterior larval tissues (Figure 1G and Table S1). These data show that Hox gene kissing occurs within PcG bodies in a PcG-dependent manner.

The BX-C Interacts Preferentially with Polycomb Enriched Regions

In order to analyze whether Hox loci only contact each other or whether they have other interacting partners in the nucleus, we developed a modified 4C protocol (see Experimental Procedures, Figure S2, and Figure S3). The *Fab-7* element from the BX-C regulates the *Abd-B* expression and plays a role in long distance interactions inside the BX-C as well as at greater genomic distances (Bantignies et al., 2003; Lanzuolo et al., 2007). Therefore, we used *Fab-7* as the 4C bait fragment in order to analyze its interaction with other loci along the 3R chromosome arm in larval brain and anterior larval discs. We found an extensive series of interactions along the 3R chromosome arm (Figure 2A). The strongest interactions occur within the BX-C. Other strong interactors are two PcG target regions, the *ss* and *srp-pnr* loci, located at a distance of 0.5 and 1 Mb, respectively (see Figure 2B). Significant interaction events are also observed at long distances. Four are particularly strong, corresponding to the NK-C, *E5/ems*, *prospero* and the ANT-C loci, and four others are weaker, corresponding to the *grn*, *hth*, *pnt*, and *Drop* loci (Figures 2A and 2C). Strikingly, all these major 4C hits are Polycomb bound regions (Schuettengruber et al., 2009). Moreover, a global analysis indicates that the 4C hits are highly enriched in Polycomb and its associated H3K27me3 repressive chromatin mark (Figure 2D).

Thus, the 4C analysis confirmed Hox gene kissing and revealed additional interactions. In order to validate the 4C results, we verified one of the strongest long-range contacts by FISH. The *lbl/lbe* genes from the NK homeobox gene complex (NK-C; Garcia-Fernandez, 2005) are located approximately 4.5 Mb distally from the BX-C (Figure 3A). They are organized in tandem and expressed in a few specialized cells in the embryonic parasegments and in the head (Jagla et al., 1997a, 1997b, 1998). The

(B) Close-up view of the 4C domainogram for the BX-C region.

(C) Close-up views for the ANT-C, NK-C and *hh-pnt* regions. Gene annotations and Pc ChIP enrichments are represented under these profiles.

(D) Distribution of Pc, H3K27me3 and H3K4me3 ChIP enrichment at non BX-C 4C hits (colored lines) and at randomly selected non-BX-C sites (gray lines). Dashed lines represent the median enrichment level, and solid lines indicate enrichment level corresponding to median ±25% of the population. See also Figure S2 and Figure S3.

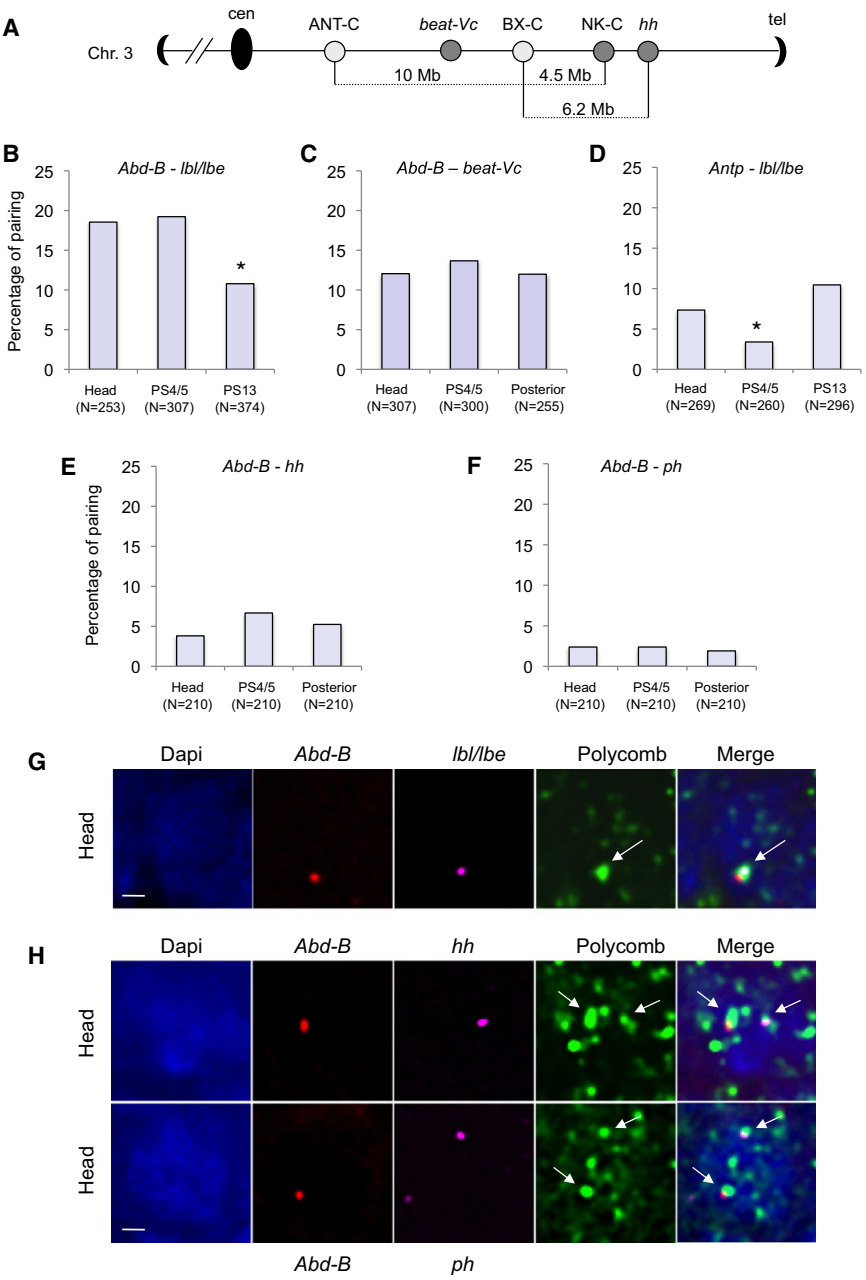

Figure 3. Specific Association between *Abd-B* and Other Target Loci

(A) Schematic drawing illustrating the chromosomal positions of the ANT-C, BX-C, NK-C, and *hh* loci on Chromosome 3R.

(B–F) Percentage colocalization between *Abd-B* and *lbl/lbe* (B), *Abd-B* and *beat-Vc* (C), *Antp* and *lbl/lbe* (D), *Abd-B* and *hh* (E), *Abd-B* and *ph*, located on Chromosome X (F). The p values of the pairwise comparison are 0.847 for Head versus PS4/5, 7.081e-03 for Head versus PS13, 2.457e-03 for PS4/5 versus PS13 (B), 0.552 for Head versus PS4/5, 0.917 for Head versus Posterior, 0.504 for PS4/5 versus Posterior (C), 0.045 for Head versus PS4/5, 0.208 for Head versus PS13, 1.411e-03 for PS4/5 versus PS13 (D), 0.189 for Head versus PS4/5, 0.481 for Head versus Posterior, 0.536 for PS4/5 versus Posterior (E), 1.0 for Head versus PS4/5, 0.736 for Head versus Posterior, 0.736 for PS4/5 versus Posterior (F). N indicates the total number of nuclei analyzed in 3–4 embryos. Asterisks indicate that the pairwise difference between samples corresponding to the left column and the other samples is significant.

(G and H) FISH-I in the embryonic heads of *Abd-B*, *lbl/lbe* and PC (G), *Abd-B*, *hh* and PC ([H], top), *Abd-B*, *ph* and PC ([H], bottom). Figure images correspond to individual nuclei of deconvolved single slices from 3D stacks. The scale bars represent 1 μm.

See also Figure S4 and Table S3.

BX-C and NK-C loci colocalized in approximately 20% of the nuclei in the head and in PS4/5 where both genes are repressed in most of the cells. This interaction decreased significantly in PS13 where *Abd-B* is active and *lbl* mostly repressed (Figure 3B and Table S3). "Ménage à trois" type of contacts among *Antp-Abd-B-lbl* are rarely observed (approximately 1% of the nuclei in embryonic heads, Figure S4), indicating that gene contacts are not all occurring simultaneously. To appreciate whether the colocalization frequency of divergently expressed PcG target genes may reflect background behavior, we then analyzed by FISH the distance between *Abd-B* and *beat-Vc*, a non-PcG target gene that lies 4.2 Mb away from *Abd-B*, a distance similar to the *lbl/lbe* locus. In all tissues, the frequencies of colocalization were similar to those observed for *Abd-B* and *lbl/lbe* in a divergently expressing tissue, while they were lower than in tissues corepressing *Abd-B* and *lbl/lbe* (Figure 3C and Table S3). This suggests that PcG-mediated silencing specifically induces gene kissing.

Gene contacts between the more remote *Antp* and *lbl/lbe* loci, which are separated by approximately 14.5 Mb, were less frequent. Nonetheless, the frequency of colocalization was significantly higher in tissues where both loci are silenced (Figure 3D and Table S3). These results confirm the observation that gene contacts between PcG target genes are more frequent when the genes are corepressed. Accordingly, as in the case of the Hox gene kissing, the contact between BX-C and NK-C occurred exclusively in a PcG body (Figure 3G).

In order to understand whether all PcG target genes associate at PcG bodies in a random manner or whether PcG-mediated gene kissing involves a subset of all target genes, we further studied by 3D-FISH the Hox gene *Abd-B* and the PcG targets *polyhomeotic* (*ph*), which is located on chromosome X, and *hedgehog* (*hh*), which is located 6.2 Mb distal to *Abd-B* on chromosome 3R (Figure 3A). The colocalization frequency was low in

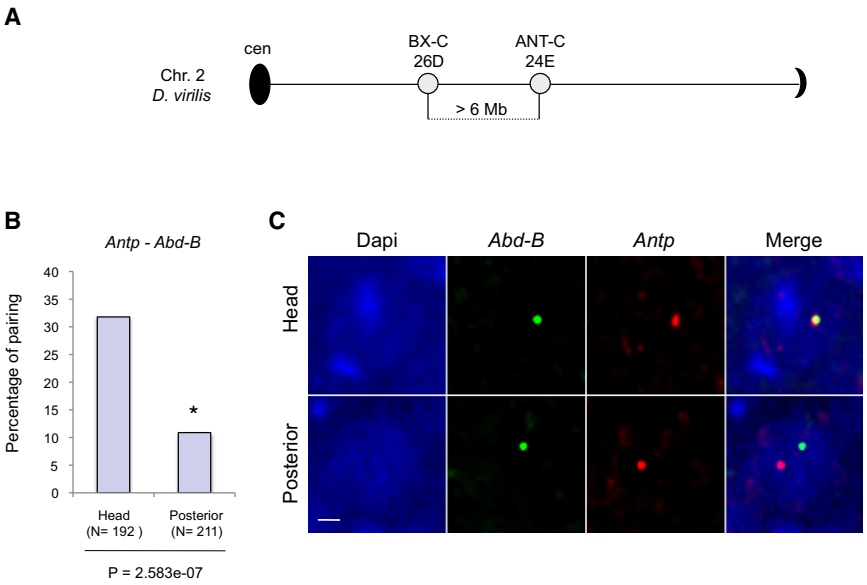

Figure 4. Conservation of Hox Gene Kissing in *D. virilis*

(A) Schematic drawing illustrating the chromosomal position of ANT-C and BX-C and their relative spacing on *D. virilis* Chromosome 2.

(B) Percentage colocalization between *Antp* and *Abd-B* in stage 11-12 *D. virilis* embryos. N indicates the total number of nuclei analyzed in three different embryos.

(C) Examples of *Antp* and *Abd-B* nuclear positions in *D. virilis*. The scale bar represents 1 μm.

See also Figure S5.

all embryonic tissues examined (Figures 3E and 3F and Table S3). In agreement with FISH analysis, no significant interaction between *hh* and *Fab-7* was detected by 4C analysis (Figure 2C). Of note, *hh* and *ph* were generally localized in smaller PC bodies than those containing the Hox genes (Figure 3H), indicating that different classes of PcG bodies exist in the nucleus. Together, these data demonstrate the existence of specific long-range associations among Hox genes and other PcG target genes, which occur within PcG nuclear bodies and correlate with their transcriptional status along the anteroposterior body axis.

Hox Gene Kissing Is Evolutionarily Conserved in *Drosophila* Species

We reasoned that, if Hox gene kissing is functionally significant, it might be conserved through evolution. Therefore, we analyzed *D.virilis*, a species separated from the *D. melanogaster* lineage 40 to 60 Myr ago. In *D. virilis*, the two Hox clusters are split between *Ubx* and *abd-A* (Von Allmen et al., 1996) instead of between *Antp* and *Ubx*. They are located on chromosome 2 and are contained within two large sequence scaffolds (13047 and 12855, see http://flybase.org/cgi-bin/gbrowse/dvir), separated by more than 6 Mb (Figure 4A). A large-scale comparison of the chromosomal organization around the Hox genes in *D. melanogaster* and *D. virilis* shows that syntenic regions of limited sizes are conserved between the two species, but the global linear organization of the chromosome is highly divergent (Figure S5A). The *D. melanogaster* counterparts of the *D. virilis* genes map to independent regions that are scattered along the entire arm of chromosome 3R. In embryo head, where both genes are repressed, *Antp* colocalized with *Abd-B* in 31% of the nuclei. In posterior segments, where *Abd-B* is active and *Antp* is repressed, the colocalization frequency was strongly reduced (Figures 4B, 4C, and Figure S5B). We conclude that, despite a radical change in linear chromosome organization, silencing-dependent Hox gene kissing is evolutionarily conserved. This suggests that this phenomenon reflects specific molecular interactions rather than a three-dimensional folding coincidence of the *D. melanogaster* 3R chromome arm.

Hox Gene Contacts Depend on Regulatory Elements in the BX-C

In transgenic systems, *Fab-7* and *Mcp* have been shown to be involved in intra- as well as interchromosomal interactions in diploid tissues (Bantignies et al., 2003, Vazquez et al., 2006). We thus analyzed Hox gene kissing in *Drosophila* lines in which *Fab-7* is deleted. The $Fab\text{-}7^{12}$ line corresponds to homozygous deletion of the *Fab-7* region containing the PRE and the chromatin boundary portion (Mihaly et al., 1997). We performed 4C in the $Fab\text{-}7^{12}$ line and compared it to the WT profile. While most of the profile is very similar (Figure 5A), some distinct differences can be seen (Figure 5B and Figure S3). In particular, the interaction with the ANT-C is significantly reduced, while the interaction with the NK-C is increased in the $Fab\text{-}7^{12}$ line (Figure 5C). We confirmed these data by FISH experiments in WT versus $Fab\text{-}7^{12}$ eye-antennal discs, showing that the colocalization frequencies are lower for *Antp-Abd-B* and higher for *Abd-B -lbl/lbe* (Figures 5D and 5E). We confirmed these effects by analyzing three more deletion lines. The $Fab\text{-}7^{1}$ and the Mcp^{1} lines correspond to homozygous deletion of *Fab-7* and *Mcp,* respectively, and the $Mcp^{H27}Fab\text{-}7^{1}$ stock corresponds to the homozygous deletion of both elements (Karch et al., 1994). In each of these lines, reduced levels of colocalization were observed between *Antp* and *Abd-B* (Figure S6).

We therefore conclude that the colocalization between the two Hox genes involves specific sequences within the *Abd-B* locus, even though these sequences do not share extensive homology with sequences from *Antp*. The finding that the deletion of *Fab-7* and *Mcp* reduces but does not abolish Hox gene kissing suggests that multiple DNA regions of the BX-C contribute to this phenomenon. This notion is corroborated by the colocalization between *Ubx* and *Antp* in posterior embryonic tissues where the *Fab-7/Mcp* region is located outside PcG bodies (Figures S1B and S1C).

Perturbation of Hox Gene Kissing Affects PcG-Dependent Silencing of the ANT-C Genes

What is the functional significance of the colocalization of silenced genes of the BX-C and the ANT-C? We have previously shown that long range interaction of homologous PRE/boundary

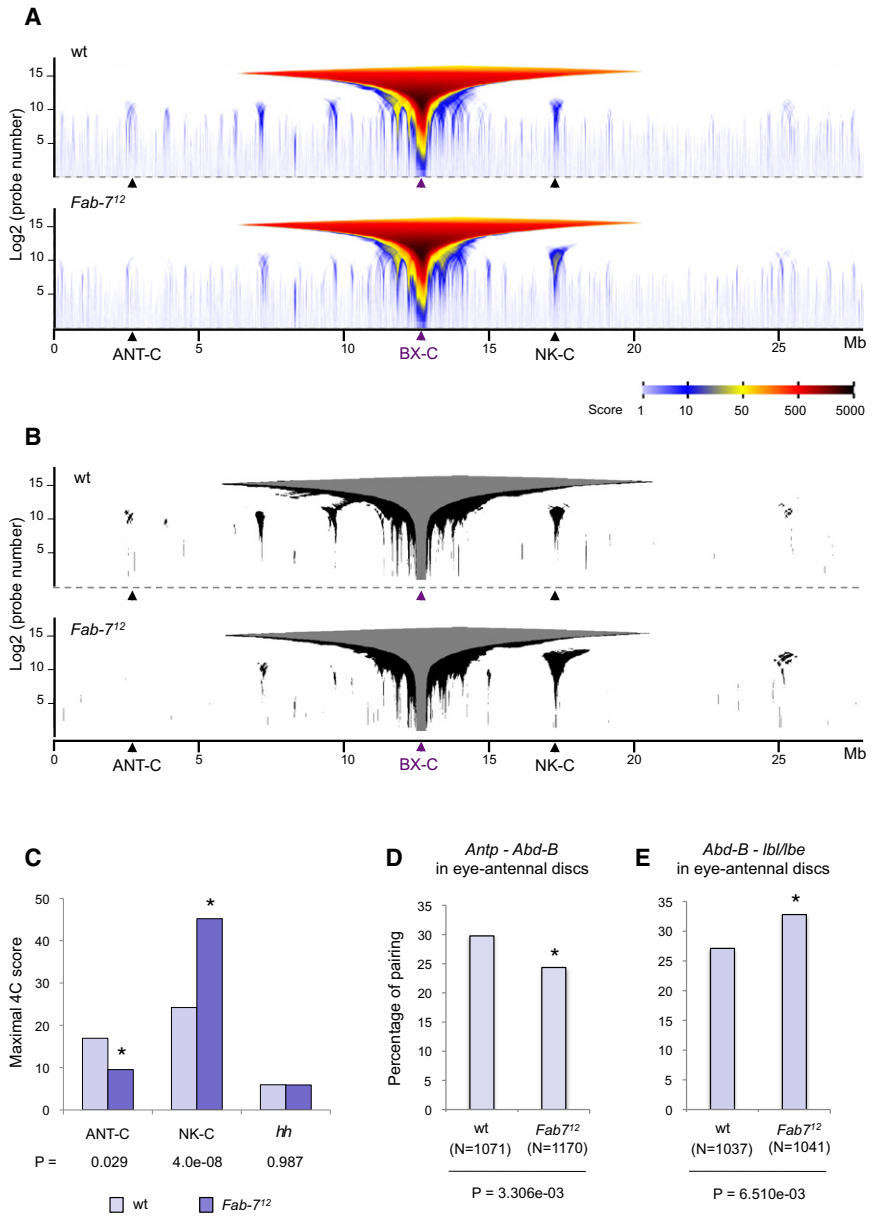

Figure 5. Hox Gene Kissing Is Partially Reduced upon Deletion of the *Fab-7* Element

(A) Whole 3R chromosome domainogram representation of wild-type and *Fab-7*^{12} 4C profiles (the 4C bait is located immediately downstream to the distal border of the deletion, allowing to directly compare WT with *Fab-7*^{12}). ANT-C, BX-C, and NK-C regions are indicated by arrowheads.

(B) Binarized domainogram representation indicating most statistically significant hits (black) outside the BX-C region. BX-C probes (gray) were excluded for the calculation.

(C) Maximal scores for WT and *Fab-7*^{12} 4C interactions within ANT-C, NK-C and *hh* regions. P values correspond to the statistical difference between WT and *Fab-7*^{12}.

(D and E) FISH in third instar larval eye-antennal discs comparing the percentage of colocalization between *Antp* and *Abd-B* (D), *Abd-B* and *lbl*/*lbe* (E) in WT versus *Fab-7*^{12}. N indicates the total number of nuclei analyzed in four antennal regions and four eye regions of the eye-antennal discs. Approximately the same numbers of nuclei were counted in both regions and the data were pooled for homogeneity and statistical analysis. P values correspond to the difference between the two populations.

See also Figure S3 and Figure S6.

elements reinforces PcG-mediated silencing (Bantignies et al., 2003). Therefore, we hypothesized that kissing between Hox genes might stabilize PcG-dependent gene silencing. In this case, we predicted that the perturbation of gene kissing in the *Fab-7*^{12} line would weaken silencing of ANT-C genes, while it should increase silencing at the NK-C locus. We measured, by reverse transcription followed by quantitative PCR (RT-qPCR) in eye-antennal discs, the level of *Abd-B*, from the BX-C, *Antp, Scr, Dfd*, and *pb* from the ANT-C, *lbe* from the NK-C and *hh* as a negative control of a gene where the frequency of contacts was not perturbed (Figures 6A and 6B). *Abd-B* was derepressed in the mutant, indicating that *Fab-7* is involved in its repression in anterior tissues, in addition to the abdominal segments of the body plan (Galloni et al., 1993; Gyurkovics et al., 1990). Strikingly, *Antp, Scr, Dfd* and *pb* were also derepressed, showing that the partial decrease in long-distance contacts induced by the deletion of *Fab-7* is sufficient to induce a decrease of silencing at the ANT-C. In contrast, the *lbe* gene, which contacts the BX-C with increased frequency, is significantly more repressed upon deletion of *Fab-7*. Finally, no effects were seen at the control *hh* gene.

Can the perturbation of gene kissing induce phenotypic changes in flies? Homeotic antenna to leg (A > L) transformation is not observed in flies carrying *Fab-7* or *Mcp* deletions. However, we reasoned that the transcriptional effect may be too subtle to induce a phenotype, and that phenotypic effects might be easier to detect in a sensitized genetic background. We thus analyzed the *Antp Nasobemia* (*Antp*^{Ns}) mutation (Talbert and Garber, 1994), in which the *Antp* P2 promoter is duplicated, inducing ectopic expression of the Antp protein in the antennal territory of larval imaginal discs and an incomplete antenna-to-leg (A > L) transformation (Figure 7A) that is sensitive to trxG and PcG functions (Vazquez et al., 1999 and data not shown). This increased expression is much lower than the WT expression of *Antp* in the wing disc, and does not correlate with altered Hox chromosome kissing (Figures S7A and S7B), suggesting that, on its own, it depends on *cis*-regulatory changes of the *Antp* locus rather than on perturbation of chromosome architecture.

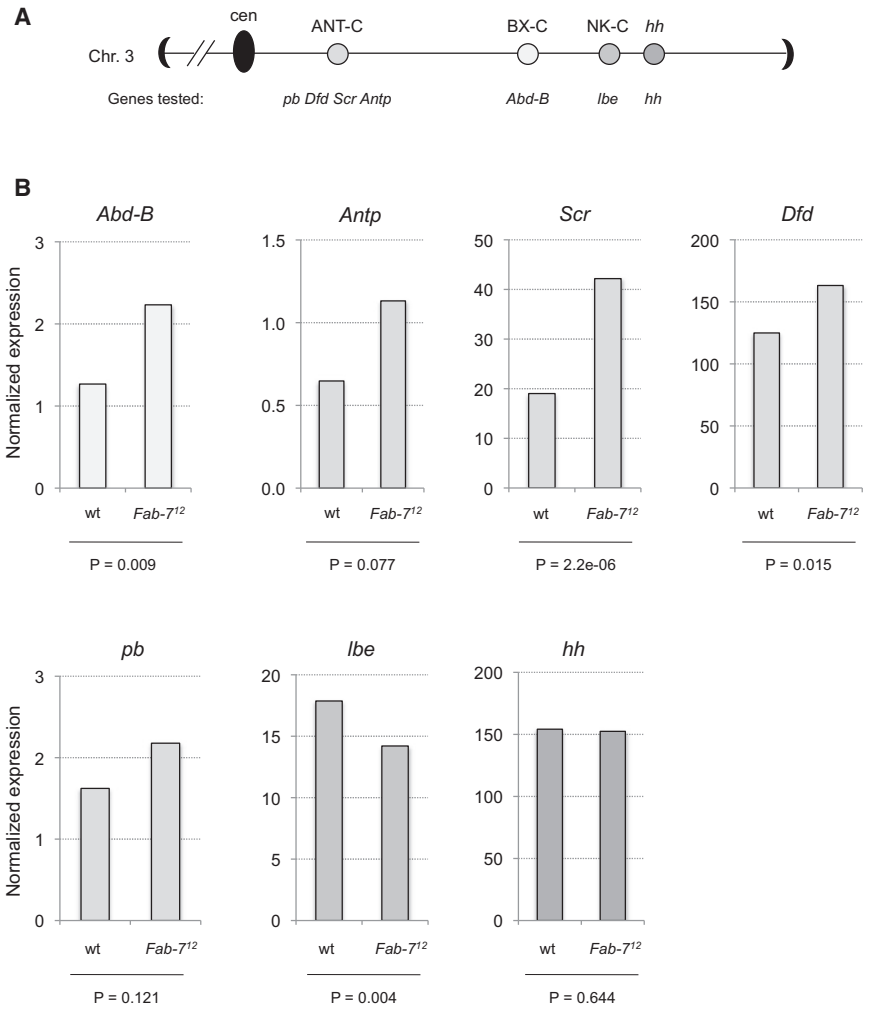

Figure 6. Transcriptional Effects at Long Distance upon Deletion of *the Fab-7* Element

(A) Schematic drawing illustrating the chromosomal positions of ANT-C, BX-C, NK-C, and the *hh* loci on chromosome 3R, with the genes from each genomic region analyzed by RT-qPCR.

(B) RT-qPCR analysis in WT and *Fab-7*^{12} lines. The results are the mean of 22 independent experiments. The statistical significances of differences between the two lines were examined by paired student tests and the p value is indicated under each graph. Note that, for genes of the ANT-C, all genes except *pb* have a p value below 0.1. The *hh* negative control is not significantly affected by the *Fab-7* deletion.

We generated different lines in which the *Antp*^{Ns} chromosome was recombined with the *Fab-7*^{12}, *Fab-7*^{1}, *Mcp*^{1}, and the *Mcp*^{H27}*Fab-7*^{1} chromosomes. As controls, the *Antp*^{Ns} chromosome was recombined with a WT chromosome from a *w*^{1118} line and with a mutant chromosome containing an *ebony* (*e*^{1}) recessive marker. Three *Antp*^{Ns}, seven *Antp*^{Ns}, *Fab-7*^{12}, seven *Antp*^{Ns}, *Fab-7*^{1}, four *Antp*^{Ns}, *Mcp*^{1}, three *Antp*^{Ns}, *Mcp*^{H27}*Fab-7*^{1} and four *Antp*^{Ns}, *e*^{1} recombinant lines were obtained and raised as balanced stocks at 21°C. No obvious differences were observed between these lines right after their establishment. However, clear differences emerged in subsequent generations, reaching a plateau after 3 to 5 generations: the *Ns* A > L phenotype was accentuated in the BX-C deletion lines (Figure 7A and Figures S7C and S7D). Transgenerational inheritance has been previously linked to PcG and trxG proteins and to the 3D organization of BX-C elements like *Fab-7* (Bantignies et al., 2003; Sollars et al., 2003). Therefore, deletions in the BX-C might enhance the A > L transformations of *Antp*^{Ns} via loss of gene contacts and progressive decrease in chromatin silencing efficiency through subsequent generations.

In addition to A > L transformations, we also observed the emergence of outgrowth phenotypes in the eye of *Antp*^{Ns} combined with *Fab-7*^{12}, *Fab-7*^{1} or *Mcp*^{H27}*Fab-7*^{1} deletions (Figure S7F). The eye phenotypes are variable, ranging from holes in the eye to large outgrowths, often emerging from ommatidia. Electron microscopy (EM) analysis of these outgrowths indicates that they resemble proximal leg or thorax-like structures, which may indicate a derepression of *Antp* in the eye imaginal discs. Eye phenotypes were observed in approximately 10% heterozygous *Antp*^{Ns}, *Mcp*^{H27}*Fab-7*^{1} and in 2% to 10% *Antp*^{Ns}, *Fab-7*^{12} and *Antp*^{Ns}, *Fab-7*^{1} adult flies for each line, but were totally absent in *Antp*^{Ns}, *Mcp*^{1} and in the recombinant control lines. Moreover, the eye outgrowths are strongly enhanced in the rare homozygous escapers, with frequencies of 60% to 80% in *Antp*^{Ns}, *Mcp*^{H27}*Fab-7*^{1}, and 25% to 60% in *Antp*^{Ns}, *Fab-7*^{12} and *Antp*^{Ns}, *Fab-7*^{1}, whereas they are observed in less than 10% in the other lines. A reduction in eye size and fused ommatidia were also observed in the *Antp*^{Ns} lines combined with BX-C deletions (Figure S7F and data not shown). Similar results were observed upon production of recombinant lines using an *Antp*^{Ns} stock, obtained from the Bloomington *Drosophila* Center. Again, these phenotypes did not appear in the two recombinant control lines obtained.

Since all these phenotypes are consistent with *Antp* derepression, we tested *Antp* expression by RT-qPCR on eye-antennal imaginal discs. Significant *Antp* derepression was observed in the *Antp*^{Ns}, *Fab-7*^{12} (Figure 7B), *Antp*^{Ns}, *Fab-7*^{1} and *Antp*^{Ns}, *Mcp*^{H27}*Fab-7*^{1} lines (Figure S7E) compared to the *Antp*^{Ns} line. In contrast, the levels of *hh* did not change significantly in the different lines.

Finally, we tested whether *Fab-7* deletion may affect phenotypes of other Hox gene mutations. We thus analyzed the heterozygous *Scr*^{4} *Scr*^{w} allele combination. This chromosome carries a null mutation (*Scr*^{4}) combined with a second mutation (*Scr*^{w})

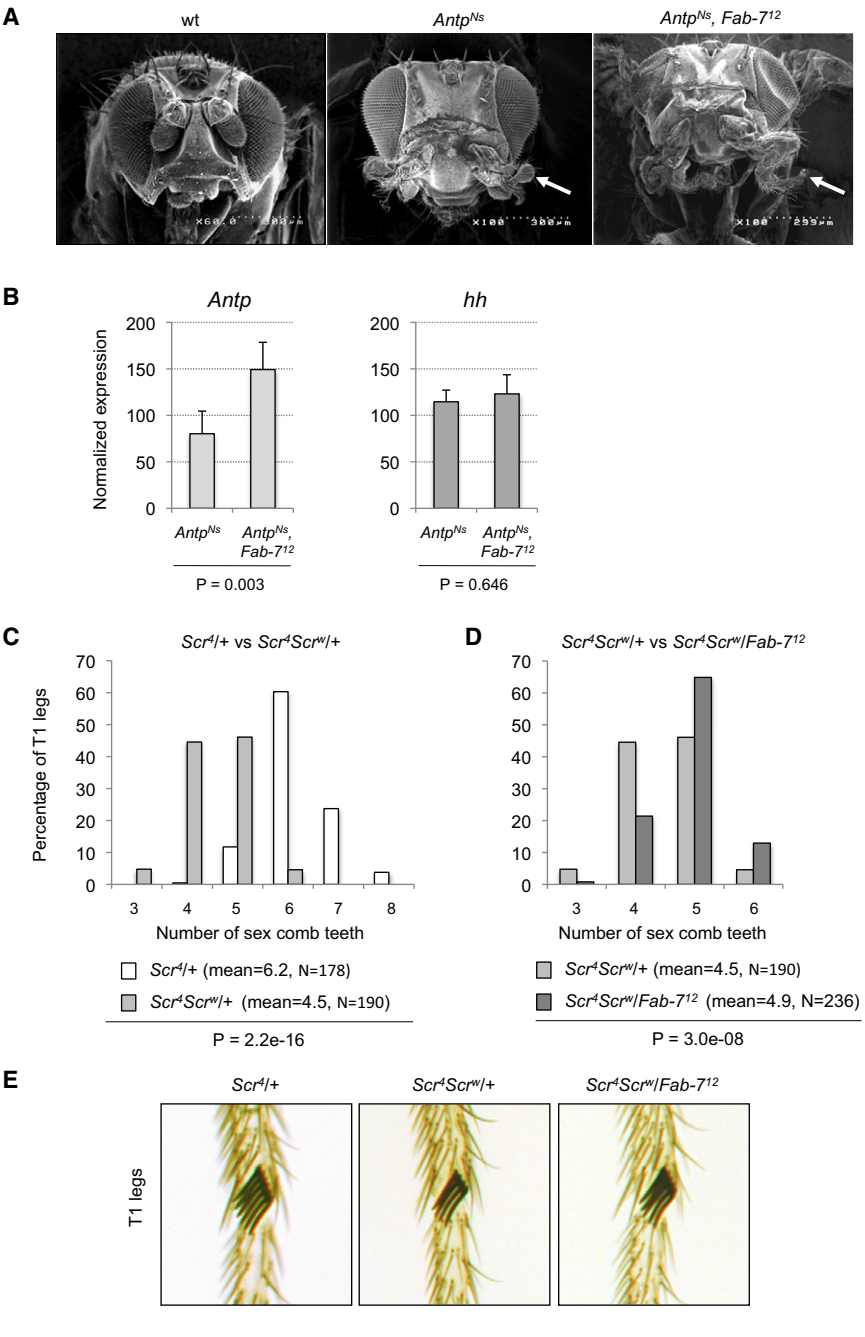

Figure 7. Deletion of *the Fab-7* Element Weakens Silencing of ANT-C Genes, Resulting in the Exacerbation of Homeotic Phenotypes in Sensitized Genetic Backgrounds

(A) Electron microscopy images showing examples of the antenna-to-leg (A > L) transformations (white arrows) in $Antp^{Ns}$ and in $Antp^{Ns}$, $Fab\text{-}7^{12}$ heterozygous flies.

(B) RT-qPCR analysis of *Antp* and *hh*. Error bars represent the standard deviation of three independent experiments.

(C and D) Distribution of the number of sex comb teeth per T1 legs in $Scr^4/+$ versus $Scr^4Scr^W/+$ (C) and in $Scr^4Scr^W/+$ versus $Scr^4Scr^W/Fab\text{-}7^{12}$ flies (D). The mean value and the N number of legs analyzed in two independent experiments are indicated. The statistical significances of differences between the distributions were examined by chi-square tests and the p value is indicated under each graph.

(E) Representative leg pictures for each genotype. See also Figure S7.

in the upstream regulatory region (Southworth and Kennison, 2002). This second mutation leads to Polycomb-dependent repression of the *Scr* gene in the first (T1) leg (Pattatucci et al., 1991 and data not shown). Whereas the $Scr^4/+$ males show an average of 6.2 sex comb teeth in the T1 leg, the additional presence of Scr^w causes a reduction to an average of 4.5, showing that the Scr^w allele represses the WT *Scr* copy in *trans* (Figures 7C and 7E). We then tested whether the deletion of *Fab-7* may attenuate this repressive effect. Crossing the Scr^4 Scr^w chromosome with the $Fab\text{-}7^{12}$ mutation induced a significant increase in the sex comb teeth (Figures 7D and 7E), showing that *Scr* is partially derepressed upon loss of the *Fab-7* element. Together, our data show that the removal of BX-C regulatory elements weakens silencing at the ANT-C, demonstrating that Hox gene kissing contributes to stabilize their corepression.

DISCUSSION

The Nature of Hox Gene Contacts

4C and FISH measurements reveal clear differences in the degree of interactions within the BX-C as opposed to those between BX-C and ANT-C genes. Earlier FISH experiments within the BX-C indicate contacts (as defined by FISH distances $\leq$ 350 nm) between the *Fab-7*/*Abd-B* and the *bxd*/*Ubx* regions in the range of 85% (Lanzuolo et al., 2007). This is much higher than the 15 to 20% observed here between *Fab-7*/*Abd-B* and *Antp* in the same tissues, i.e., head of the embryo (Figure 1B). These FISH data are concordant with 4C, where the signals within the BX-C are far stronger than those between *Fab-7* and the ANT-C. Therefore, the higher-order interactions between elements of the BX-C are tighter than those between heterologous loci such as the BX-C and the ANT-C. We propose that this reflects a hierarchy of higher-order structures in the nucleus, where chromatin elements are much more likely to interact with neighboring partners in *cis* before engaging in interactions with remote partners. A 3D loop-structure model has been proposed for the BX-C (Lanzuolo et al., 2007). These structures may be highly dynamic entities enabling contacts

between epigenetic elements from distant loci when they come into three-dimensional proximity in the same nuclear compartment.

The Discovery of a 3D Polycomb Interactome Gene Network

Our 4C analysis clearly reveals that the gene kissing is not limited to Hox genes, since we found that the BX-C is engaged in additional contacts with other partners on the same chromosome arm. The fact that all the main interaction partners are PcG-bound chromatin domains, suggests that PcG proteins contribute to the establishment of long-range contacts among their target genes in the 3D nuclear space. However, most PcG target genes are cobound by many other chromatin factors, including insulator proteins like CTCF and Su(Hw) (Bushey et al., 2009; Negre et al., 2010), and these proteins may contribute to drive long-distance contacts via chromatin boundary or insulator elements present at PcG target loci.

The 4C analysis measured chromosome contact frequencies from a large population of fixed cells, however it cannot distinguish whether these interactions are simultaneous. Two-color FISH experiments validated 4C contacts between BX-C and ANT-C and between BX-C and NK-C. Three-color FISH experiments, where all three complexes are silenced, revealed that the contacts are not simultaneous, at least during embryogenesis (Figure S4). We thus propose that each of the Hox loci is in dynamic contact with the other one, as well as with other PcG target loci. The existence of multiple gene contacts as we discovered in 4C and FISH can thus explain why the two Hox loci do not interact in all nuclei, but only in a significant minority of them. Interestingly, the deletion of *Fab-7* reduced *Antp-Abd-B* contacts while it increased *Abd-B-Ibl* contacts. This might suggest that, once free from one interacting partner, *Abd-B* chromatin might be available for increased interactions with some of the other partners. In the future, further 4C studies and high-throughput FISH analysis with probes directed against the interacting 4C loci and the intervening regions should extend these observations to gain a systematic understanding of Polycomb dependent gene kissing. In this context, a study which combined 3C and ChIP (called 6C) using antibodies against the human PcG protein EZH2 revealed intra- and inter-chromosomal interactions between PcG-bound elements (Tiwari et al., 2008). Although that study analyzed a small number of interactions, it raises the possibility that a hard-wired Polycomb target gene network may also exist in vertebrates.

Evolutionary Conservation and Functional Significance of Hox Gene Kissing

The evolutionary conservation of Hox gene kissing between *D. melanogaster* and *D. virilis* strongly suggests that selective pressure maintains the spatial proximity of Hox complexes. This fact reinforces the idea that gene kissing might stabilize PcG-mediated silencing of Hox genes, contributing to the specification of body structures along the anteroposterior axis. *Fab-7* and *Mcp* might represent examples of bifunctional regulatory elements, as they appear to have two distinct roles: on the one hand, they regulate the expression of their flanking genes in *cis* and, on the other, they mediate long-distance regulatory interactions with Hox genes in the ANT-C. We propose that one of the roles of *Fab-7* and *Mcp* was to promote locus-wide chromatin condensation of the ancestral Hox gene cluster by interacting with more anterior genes. The maintenance of these interactions after the physical split of the cluster may have originated the long-distance pairing that is still observed today.

The analysis of deletions of BX-C elements reveals important features of long-range regulation. Within the BX-C, we noticed that the removal of *Fab-7* reduces PcG-dependent silencing of the *abd-A* and *Ubx* genes (2- to 3-fold derepression, data not shown). This result indicates that multiple regulatory interactions take place for the strong and faithful repression of the BX-C in anterior segments. In this system, we exclude secondary effects in *trans* of *Abd-B* on *Ubx* and *abd-A* because the products of posterior Hox genes always repress, not activate, more anterior genes (a phenomenon called posterior dominance, Kuziora, 1993; Struhl and White, 1985). Indeed, this feature might attenuate the transcriptional effects of loss of long-distance Hox contacts.

A second level of higher-order chromatin association involves larger scales, such as between the BX-C and ANT-C loci. These contacts are probably not indispensable for repression. For instance, *Antp* is silenced in every anterior cell, even if it contacts the BX-C in a minority of the nuclei. *Cis* regulatory elements are probably able to maintain silencing to a sufficient degree. However, small but clear transcriptional derepression of multiple ANT-C genes was observed upon mutations in the BX-C. In this context, one should note that the BX-C contacts many other loci in addition to the ANT-C. Likewise, the ANT-C may contact several other PcG target regions. These other contacts could functionally complement a loss of pairing upon BX-C mutations. ANT-C may maintain spatial association with other regions within the BX-C or with other domains that participate in the same spatial network of PcG target genes, thus remaining in an appropriate regulatory environment. However, this compensation cannot be complete, as illustrated by the increase in homeotic phenotypes seen in the sensitized *Antp* and *Scr* backgrounds. To our knowledge, this is the first report that links the function of a chromatin element involved in 3D chromosome contacts to specific phenotypes.

Hox Contacts and Chromosomal Rearrangements

Three different splitting events of the ancestral Hox gene complex have been detected to date in the *Drosophila* genus. Two of them, mentioned in this study, are represented by the separation of *Antp* and *Ubx* in *D. melanogaster* and of *Ubx* and *abd-A* in *D. virilis*. A third split has been described in *D. buzzatii* (Negre et al., 2003). This species, a member of the *D. repleta* group, shows a split between *Ubx* and *abd-A* as with *D. virilis* (Ranz et al., 1997), and an additional split, whereby the most anterior gene, *lab*, has been relocated flanking the two posterior Hox genes *abd-A* and *Abd-B*. In light of our data, the most likely scenario that might explain this third split involves translocation of the entire *lab* locus to the border of the posterior cluster due to PcG-dependent spatial proximity between the anterior and posterior Hox clusters. Related to this point, in mammalian cells the proximity of chromosome or chromosomal loci has been suggested to induce chromosomal rearrangements between

them (Branco and Pombo, 2006; Lin et al., 2009; Nikiforova et al., 2000; Roix et al., 2003). Moreover, chromosome kissing events dependent on colocalization in transcription factories were also shown to be correlated with a high rate of translocation (Osborne et al., 2007). It is interesting to note that Hox gene clusters have been submitted to considerable rearrangements during evolution of the animal kingdom (Garcia-Fernandez, 2005). We propose that split Hox clusters might have contributed to evolution of chromosomes bearing them.

In conclusion, the data described here show that the specific nuclear organization imposed by the PcG proteins in *Drosophila* diploid tissues influences the maintenance of epigenetic states and might contribute to genome evolution.

EXPERIMENTAL PROCEDURES

Fly Stocks and Handling

Flies were raised in standard cornmeal yeast extract media at 25°C. The Oregon-R w^{1118} line was used as wild-type (WT) *D. melanogaster*. A *w* stock (#15010-1051.17, from the Tucson species stock center) was used as WT *D. virilis*. The Pcl^{10}/ *KrGFP-CyO* stock was used for selection of homozygous Pcl^{10} mutants (Bantignies et al., 2003). A Pc^{XL5}/ *KrGFP-TM3,Sb* stock was used for the selection of homozygous Pc^{XL5} mutants. The $Fab\text{-}7^{12}$, $Fab\text{-}7^{1}$, Mcp^{1}, and $Mcp^{H27}Fab\text{-}7^{1}$ deletion lines were described in (Karch et al., 1994; Mihaly et al., 1997). The $Antp^{Ns}$ stock used in this study was provided by W. Gehring. $Antp^{Ns}$ stock from Bloomington was also used, although this stock shows lower penetrance of the A > L phenotype. All the $Antp^{Ns}$ recombinant lines were maintained over the *KrGFP-TM3,Sb* balancer (from stocks BL#5195 of the Bloomington *Drosophila* Stock Center). The *ebony* (e^{1}), Scr^{4} and $Scr^{4}Scr^{W}$ stocks were from Bloomington (BL#2558, BL#2188 and BL#809, respectively). Staged eggs were collected on agar plates with standard vinegar/fresh yeast medium. *Antp* and *Scr* mutant Flies were grown at 21°C, and sex comb teeth were counted under a Nikon SMZ1000 binocular at 80× magnification.

RT-qPCR

Third-instar larval imaginal eye-antennal discs were dissected in Schneider's *Drosophila* Medium (GIBCO) and 30–40 discs were taken for RNA isolation using TRIzol reagent (Invitrogen). 300–400 ngs of total RNA were used for the RT reaction. RT was performed using the Superscript III First Strand Synthesis Kit from Invitrogen following the manufacturer's instructions and using hexamer primers. cDNA quantifications were performed by real-time PCR, using a Roche Light Cycler and the Light Cycler FastStart DNA Master SYBR green I kit. NdeI digested genomic DNA served for the standard curve. Expression levels were normalized to Rp49 and multiplied by 1.10^{4}. Primer sequences are listed in Table S4.

Two-Color 3D-FISH and FISH-I

These procedures are described in the Extended Experimental Procedures.

Microscopy and Image Analysis

Microscopy and 3D image analysis were as previously described (Bantignies et al., 2003). Minor modifications and EM are described in the Extended Experimental Procedures.

Chromosome Conformation Capture on Chip (4C)

Flies were grown at 25°C. Third-instar larval brain and anterior discs from 200 larvae were dissected in Schneider's *Drosophila* Medium and used for the 3C. The 3C was performed as previously described (Hagege et al., 2007; Miele and Dekker, 2009) with the main differences being the use of DpnII (New England Biolabs), a 4 bp cutter restriction enzyme, and a fixation in 3% para-formaldehyde for 30 min, maximizing sensitivity and resolution of contact detection. The 4C method includes an "anchor biotinylated primer extension" procedure that is described in detail in the Extended Experimental Procedures. Microarray analyses are described in the same section and Figure S2 and Figure S3.

SUPPLEMENTAL INFORMATION

Supplemental Information includes Extended Experimental Procedures, seven figures, and six tables and can be found with this article online at doi:10.1016/j.cell.2010.12.026.

ACKNOWLEDGMENTS

We would like to thank W. Gehring, F. Karch, H. Gyurkovics, J.M. Dura, and Alain Pelisson for fly lines and plasmids. We also thank T. Sexton and D. Cribbs for stimulating discussions; B. Pfeiffer and S. Celniker for sharing the *D. virilis* BX-C sequence before publication; Chantal Cazevieille for electron microscopy at the Centre de Ressources en Imagerie Cellulaire of Montpellier. F.B. is supported by the CNRS; V.R. and I.C. were supported by the Ministère de l'Enseignement Supérieur, the Association pour la Recherche sur le Cancer, and the Agence Nationale de la Recherche. B.L. was supported by the Ministère de l'Enseignement Supérieur. B.S. was supported by the Fondation de la Recherche Médicale. G.C. was supported by grants of the CNRS, the Human Frontier Science Program Organization, the European Union FP6 (Network of Excellence, The Epigenome, and STREP 3D Genome), the European Research Council (ERC-2008-AdG No 232947), by the Indo-French Centre for Promotion of Advanced Research, by the Agence Nationale de la Recherche, and by the Ministère de l'Enseignement Supérieur, ACI BCMS.

Received: June 22, 2009
Revised: September 22, 2010
Accepted: December 17, 2010
Published: January 20, 2011

REFERENCES

Alkema, M.J., Bronk, M., Verhoeven, E., Otte, A., van 't Veer, L.J., Berns, A., and van Lohuizen, M. (1997). Identification of Bmi1-interacting proteins as constituents of a multimeric mammalian polycomb complex. Genes Dev. *11*, 226–240.

Bantignies, F., Grimaud, C., Lavrov, S., Gabut, M., and Cavalli, G. (2003). Inheritance of Polycomb-dependent chromosomal interactions in Drosophila. Genes Dev. *17*, 2406–2420.

Branco, M.R., and Pombo, A. (2006). Intermingling of chromosome territories in interphase suggests role in translocations and transcription-dependent associations. PLoS Biol. *4*, e138.

Buchenau, P., Hodgson, J., Strutt, H., and Arndt-Jovin, D.J. (1998). The distribution of polycomb-group proteins during cell division and development in Drosophila embryos: impact on models for silencing. J. Cell Biol. *141*, 469–481.

Bushey, A.M., Ramos, E., and Corces, V.G. (2009). Three subclasses of a Drosophila insulator show distinct and cell type-specific genomic distributions. Genes Dev. *23*, 1338–1350.

Castelli-Gair, J. (1998). Implications of the spatial and temporal regulation of Hox genes on development and evolution. Int. J. Dev. Biol. *42*, 437–444.

Cavalli, G. (2007). Chromosome kissing. Curr. Opin. Genet. Dev. *17*, 443–450.

Duncan, I. (1987). The bithorax complex. Annu. Rev. Genet. *21*, 285–319.

Fedorova, E., Sadoni, N., Dahlsveen, I.K., Koch, J., Kremmer, E., Eick, D., Paro, R., and Zink, D. (2008). The nuclear organization of Polycomb/Trithorax group response elements in larval tissues of Drosophila melanogaster. Chromosome Res. *16*, 649–673.

Fraser, P., and Bickmore, W. (2007). Nuclear organization of the genome and the potential for gene regulation. Nature *447*, 413–417.

Galloni, M., Gyurkovics, H., Schedl, P., and Karch, F. (1993). The bluetail transposon: evidence for independent *cis*-regulatory domains and domain boundaries in the bithorax complex. EMBO J. *12*, 1087–1097.

Garcia-Fernandez, J. (2005). The genesis and evolution of homeobox gene clusters. Nat. Rev. Genet. *6*, 881–892.

Grimaud, C., Bantignies, F., Pal-Bhadra, M., Ghana, P., Bhadra, U., and Cavalli, G. (2006). RNAi Components Are Required for Nuclear Clustering of Polycomb Group Response Elements. Cell *124*, 957–971.

Gyurkovics, H., Gausz, J., Kummer, J., and Karch, F. (1990). A new homeotic mutation in the Drosophila bithorax complex removes a boundary separating two domains of regulation. EMBO J. *9*, 2579–2585.

Hagege, H., Klous, P., Braem, C., Splinter, E., Dekker, J., Cathala, G., de Laat, W., and Forne, T. (2007). Quantitative analysis of chromosome conformation capture assays (3C-qPCR). Nat. Protoc. *2*, 1722–1733.

Jagla, K., Frasch, M., Jagla, T., Dretzen, G., Bellard, F., and Bellard, M. (1997a). ladybird, a new component of the cardiogenic pathway in Drosophila required for diversification of heart precursors. Development *124*, 3471–3479.

Jagla, K., Jagla, T., Heitzler, P., Dretzen, G., Bellard, F., and Bellard, M. (1997b). ladybird, a tandem of homeobox genes that maintain late wingless expression in terminal and dorsal epidermis of the Drosophila embryo. Development *124*, 91–100.

Jagla, T., Bellard, F., Lutz, Y., Dretzen, G., Bellard, M., and Jagla, K. (1998). ladybird determines cell fate decisions during diversification of Drosophila somatic muscles. Development *125*, 3699–3708.

Karch, F., Galloni, M., Sipos, L., Gausz, J., Gyurkovics, H., and Schedl, P. (1994). *Mcp* and *Fab-7*: molecular analysis of putative boundaries of *cis*-regulatory domains in the bithorax complex of *Drosophila melanogaster*. Nucleic Acids Res. *22*, 3138–3146.

Kaufman, T.C., Seeger, M.A., and Olsen, G. (1990). Molecular and genetic organization of the antennapedia gene complex of Drosophila melanogaster. Adv. Genet. *27*, 309–362.

Kosman, D., Mizutani, C.M., Lemons, D., Cox, W.G., McGinnis, W., and Bier, E. (2004). Multiplex detection of RNA expression in Drosophila embryos. Science *305*, 846.

Kuziora, M.A. (1993). Abdominal-B protein isoforms exhibit distinct cuticular transformations and regulatory activities when ectopically expressed in Drosophila embryos. Mech. Dev. *42*, 125–137.

Lanzuolo, C., Roure, V., Dekker, J., Bantignies, F., and Orlando, V. (2007). Polycomb response elements mediate the formation of chromosome higher-order structures in the bithorax complex. Nat. Cell Biol. *9*, 1167–1174.

Lewis, E.B., Pfeiffer, B.D., Mathog, D.R., and Celniker, S.E. (2003). Evolution of the homeobox complex in the Diptera. Curr. Biol. *13*, R587–R588.

Lin, C., Yang, L., Tanasa, B., Hutt, K., Ju, B.G., Ohgi, K., Zhang, J., Rose, D.W., Fu, X.D., Glass, C.K., et al. (2009). Nuclear receptor-induced chromosomal proximity and DNA breaks underlie specific translocations in cancer. Cell *139*, 1069–1083.

Merdes, G., and Paro, R. (2009). About combs, notches, and tumors: epigenetics meets signaling. Dev. Cell *17*, 440–442.

Messmer, S., Franke, A., and Paro, R. (1992). Analysis of the functional role of the Polycomb chromo domain in Drosophila melanogaster. Genes Dev. *6*, 1241–1254.

Miele, A., and Dekker, J. (2009). Mapping Cis- and Trans- Chromatin Interaction Networks Using Chromosome Conformation Capture (3C). Methods Mol. Biol. *464*, 105–121.

Mihaly, J., Hogga, I., Gausz, J., Gyurkovics, H., and Karch, F. (1997). In situ dissection of the Fab-7 region of the bithorax complex into a chromatin domain boundary and a Polycomb-response element. Development *124*, 1809–1820.

Morata, P., Jimenez-Mesa, J., Nunez de Castro, I., and Sanchez-Jimenez, F.M. (1994). Vinca alkaloids enhance the half-life of tumour ornithine decarboxylase. Cancer Lett. *81*, 209–213.

Muller, J., and Verrijzer, P. (2009). Biochemical mechanisms of gene regulation by polycomb group protein complexes. Curr. Opin. Genet. Dev. *19*, 150–158.

Muller, M., Hagstrom, K., Gyurkovics, H., Pirrotta, V., and Schedl, P. (1999). The mcp element from the Drosophila melanogaster bithorax complex mediates long-distance regulatory interactions. Genetics *153*, 1333–1356.

Negre, B., Ranz, J.M., Casals, F., Caceres, M., and Ruiz, A. (2003). A new split of the Hox gene complex in Drosophila: relocation and evolution of the gene labial. Mol. Biol. Evol. *20*, 2042–2054.

Negre, N., Brown, C.D., Shah, P.K., Kheradpour, P., Morrison, C.A., Henikoff, J.G., Feng, X., Ahmad, K., Russell, S., White, R.A., et al. (2010). A comprehensive map of insulator elements for the Drosophila genome. PLoS Genet. *6*, e1000814.

Nikiforova, M.N., Stringer, J.R., Blough, R., Medvedovic, M., Fagin, J.A., and Nikiforov, Y.E. (2000). Proximity of chromosomal loci that participate in radiation-induced rearrangements in human cells. Science *290*, 138–141.

Okamoto, I., and Heard, E. (2009). Lessons from comparative analysis of X-chromosome inactivation in mammals. Chromosome Res. *17*, 659–669.

Osborne, C.S., Chakalova, L., Mitchell, J.A., Horton, A., Wood, A.L., Bolland, D.J., Corcoran, A.E., and Fraser, P. (2007). Myc dynamically and preferentially relocates to a transcription factory occupied by Igh. PLoS Biol. *5*, e192.

Pattatucci, A.M., Otteson, D.C., and Kaufman, T.C. (1991). A functional and structural analysis of the Sex combs reduced locus of Drosophila melanogaster. Genetics *129*, 423–441.

Pirrotta, V., Chan, C.S., McCabe, D., and Qian, S. (1995). Distinct parasegmental and imaginal enhancers and the establishment of the expression pattern of the Ubx gene. Genetics *141*, 1439–1450.

Ranz, J.M., Segarra, C., and Ruiz, A. (1997). Chromosomal homology and molecular organization of Muller's elements D and E in the Drosophila repleta species group. Genetics *145*, 281–295.

Ren, X., Vincenz, C., and Kerppola, T.K. (2008). Changes in the distributions and dynamics of polycomb repressive complexes during embryonic stem cell differentiation. Mol. Cell. Biol. *28*, 2884–2895.

Roix, J.J., McQueen, P.G., Munson, P.J., Parada, L.A., and Misteli, T. (2003). Spatial proximity of translocation-prone gene loci in human lymphomas. Nat. Genet. *34*, 287–291.

Saurin, A.J., Shiels, C., Williamson, J., Satijn, D.P., Otte, A.P., Sheer, D., and Freemont, P.S. (1998). The human polycomb group complex associates with pericentromeric heterochromatin to form a novel nuclear domain. J. Cell Biol. *142*, 887–898.

Schuettengruber, B., Chourrout, D., Vervoort, M., Leblanc, B., and Cavalli, G. (2007). Genome Regulation by Polycomb and Trithorax Proteins. Cell *128*, 735–745.

Schuettengruber, B., Ganapathi, M., Leblanc, B., Portoso, M., Jaschek, R., Tolhuis, B., van Lohuizen, M., Tanay, A., and Cavalli, G. (2009). Functional Anatomy of Polycomb and Trithorax Chromatin Landscapes in Drosophila Embryos. PLoS Biol. *7*, e13.

Sexton, T., Bantignies, F., and Cavalli, G. (2009). Genomic interactions: chromatin loops and gene meeting points in transcriptional regulation. Semin. Cell Dev. Biol. *20*, 849–855.

Sexton, T., Umlauf, D., Kurukuti, S., and Fraser, P. (2007). The role of transcription factories in large-scale structure and dynamics of interphase chromatin. Semin. Cell Dev. Biol. *18*, 691–697.

Sollars, V., Lu, X., Xiao, L., Wang, X., Garfinkel, M.D., and Ruden, D.M. (2003). Evidence for an epigenetic mechanism by which Hsp90 acts as a capacitor for morphological evolution. Nat. Genet. *33*, 70–74.

Southworth, J.W., and Kennison, J.A. (2002). Transvection and silencing of the Scr homeotic gene of Drosophila melanogaster. Genetics *161*, 733–746.

Struhl, G., and White, R.A. (1985). Regulation of the Ultrabithorax gene of Drosophila by other bithorax complex genes. Cell *43*, 507–519.

Talbert, P.B., and Garber, R.L. (1994). The Drosophila homeotic mutation Nasobemia (AntpNs) and its revertants: an analysis of mutational reversion. Genetics *138*, 709–720.

Tiwari, V.K., Cope, L., McGarvey, K.M., Ohm, J.E., and Baylin, S.B. (2008). A novel 6C assay uncovers Polycomb-mediated higher order chromatin conformations. Genome Res. *18*, 1171–1179.

Vazquez, J., Muller, M., Pirrotta, V., and Sedat, J.W. (2006). The Mcp element mediates stable long-range chromosome-chromosome interactions in Drosophila. Mol. Biol. Cell *17*, 2158–2165.

Vazquez, M., Moore, L., and Kennison, J.A. (1999). The trithorax group gene osa encodes an ARID-domain protein that genetically interacts with the brahma chromatin-remodeling factor to regulate transcription. Development *126*, 733–742.

Von Allmen, G., Hogga, I., Spierer, A., Karch, F., Bender, W., Gyurkovics, H., and Lewis, E. (1996). Splits in fruitfly Hox gene complexes. Nature *380*, 116.

Williams, A., Spilianakis, C.G., and Flavell, R.A. (2010). Interchromosomal association and gene regulation in trans. Trends Genet. *26*, 188–197.